Indian Journal of Chemistry
Vol. 64, June 2025, pp. 557-570
DOI: 10.56042/ijc.v64i6.9991

Synthesis, DNA binding, and dual topoisomerase I/II inhibitory activities of $[Ru(tpy)(adtpy)]^{2+}$ and $[Ru(dtp)(adtpy)]^{2+}$

Jun-Feng Kou[a,b]

[a] College of Chemistry and Chemical Engineering, Yunnan Normal University, Kunming, Yunnan, 650500, P. R. China

[b] MOE Laboratory of Bioinorganic and Synthetic Chemistry, State Key Laboratory of Optoelectronic Materials and Technologies, School of Chemistry and Chemical Engineering, Sun Yat-Sen University, Guangzhou 510275, P. R. China

E-mail: kjf416@163.com

Received 29 March 2024; accepted (revised) 22 January 2025

Two ruthenium (II) complexes $[Ru(tpy)(adtpy)]^{2+}$ (**1**) and $[Ru(dtp)(adtpy)]^{2+}$ (**2**) have been synthesized and characterized. The DNA-binding behavior of complexes have been studied by using spectroscopic and viscosity measurements. Results suggest that two of the complexes bind to DNA in an intercalative mode. Topoisomerase inhibition and DNA strand passage assay confirmed that two Ru (II) complexes act as efficient dual inhibitors of topoisomerases I and II by interference with the DNA religation. In MTT cytotoxicity studies, two Ru (II) complexes exhibit antitumor activity against BEL-7402, HeLa, MCF-7 and HepG2 tumor cells. Flow cytometry analysis shows an increase in the percentage of cells with apoptotic morphological features in the sub-G1 phase for Ru (II) complexes. Apoptosis induction has also been observed from AO/EB staining assay and Annexin V-FITC/PI double staining.

Keywords: Ruthenium (II) complex; DNA-binding; Topoisomerase inhibition; Cytotoxicity; Apoptosis

DNA topoisomerases are essential for the processes of chromosomal segregation and relaxation of DNA during replication and transcription, and may also be required for recombination by transiently breaking one or two strands of DNA, passing a single- or double-stranded DNA through the break, and finally resealing the break[1]. Although the biological functions of Topoisomerases are important for ensuing genomic integrity, many studies have shown that the ability to interfere with enzymes or generate enzyme-mediated damage is an effective strategy for cancer therapy[2], including camptothecin (CPT)[2a], indolocarbazole[2b], indenoisoquinoline[2c] and phenanthridine[2d] derivatives inhibiting Topo I, Etoposide (VP-16)[2e], Doxorubicin[2f], anthracyclines[2g], aminoacridines[2h], and ellipticines[2i] targeting Topo II.

As cancer involves multiple pathogenic factors[3], alterations to the regulation of one Topo are often compensated by alterations in the other. Consequently, only topoisomeraseIor II-directed agents have no good efficiency in the clinic, current anticancer therapies.

On the other hand, the results from experimental trials with simultaneous or sequential exposure of tumour cells to Etoposide[2e] and to Topotecan[4] or Irinotecan[5] demonstrated an antagonistic, rather than synergistic, behaviour including typically severe to life-threatening neutropenia and anemia[6]. So dual Topo I and Topo II- targeting drugs may be a more promising anti-tumour activity[7].

During the past decade, some naturally occurring and synthetic compounds have been found to inhibit both topoisomerases[8], such as TAS-103 (Ref. 8b), Prodigiosin[27c], Benzothiopyranoindoles[8d], intoplicine[8e], XR5000 (DACA)[8f], and Triptycene Bisquinones[8g]. However, the vast majority of such studies have been focused on organic compounds and, to a far lesser extent, on metal complexes.

Recently, ruthenium complexes have received considerable attention as topoisomerase inhibitors due to their rich photochemical properties and varied coordination forms.

Considering the affinitive relationship between DNA intercalators and topoisomerase inhibitors, intercalative Ru (II) polypyridyl complexes are undoubtedly expectable for serving as a new class of topoisomerase inhibitors, and of further valuable as antitumor drugs. However, study involving the dual inhibition of Topo I and II by Ru (II) polypyridyl complexes is rare. Only some Ru (II) complexes were found to act as efficient dual inhibitors of Topo I and II (Ref. 9), such as[$[Ru(bpy)_2(bfipH)]^{2+}$ and

$[Ru(phen)_2(bfipH)]^{2+}$ (bpy = 2,2-bipyridine, phen = 1,10-phenanthroline, bfipH = 2-(benzofuran-2-yl)imidazo[4,5-f][1,10]phenanthroline) [9a]. Two chiral Ru (II) complexes, Δ- and Λ-$[Ru(bpy)_2(ipad)]^{2+}$ (ipad = 2-(anthracene-9,10-dione-2-yl) imidazo[4,5-f] [1,10]phenanthroline)[9b], bearing an anthraquinone group, a series of chiral Ru (II) complexes with phenolic hydroxyl groups[9c], four furan bearing chiral Ru (II) complexes Δ- and Λ-enantiomers of $[Ru(bpy)_2(pocl)]^{2+}$ (pocl=2-(5-cholrofuran-9,10-dione-2-yl)imidazo[4,5-f][1,10] phenanthroline) and $[Ru(bpy)_2$ $(poi)]^{2+}$(poi=2-(5-iodofuran-9,10-dione-2-yl) imidazo[4,5-f][1,10]phenanthroline)[9d] and Ru (II) complexes containing1,1-(pyrazin-2-yl)pyreno[4,5-e][1,2,4]Triazine[9e], Ru (II) complexes containing asymmetric tridentate ligands, $([Ru(dtzp)(dppt)]^{2+}$, $[Ru(dtzp)(pti)]^{2+}$, $Ru(dtzp)(ptn)]^{2+}$, $[Ru(dtzp)(pta)]^{2+}$ and $[Ru(dtzp)(ptp)]^{2+}$ (dtzp is 2,6-di(thiazol-2-yl) pyridine, dppt is 3-(1,10-phenanthroline-2-yl)-5, 6-diphenyl-as-triazine), pti is 3-(1,10-phenanthroline-2-yl)-as-triazino-[5,6-f]isatin, ptn is 3-(1,10-phenanthroline-2-yl)-as-triazino[5,6-f]naphthalene, pta is 3-(1,10-phenanthroline-2-yl)-as-triazino[5,6-f] acenaphthylene, and ptp is 3-(1,10-phenanthroline-2-yl)-as-triazino[5,6-f] -phenanthrene)][9f].

In the present study, we designed and synthesized two ruthenium (II) complexes $[Ru(tpy)adtpy]^{2+}$ and $[Ru(dtp)adtpy]^{2+}$ (adtpy = 4'-(2-Anthryl)-2,2':6',2''-terpyridine) bearing anthraquinone group. They were demonstrated to efficiently inhibit both of Topo I and II, and induce the apoptosis of cell, which was investigated by MTT assay, real-time cell growth and proliferation assay, AO/EB staining, Annexin V-FITC/PI Double Staining and cell cycle analysis. which indicates that they may be promising chemotherapeutic drugs for cancer.

Experimental Section

DNA-Binding Experiments

The DNA-binding experiments were performed at RT. All spectroscopic titrations and viscosity measurements were carried out in buffer A (5 mM Tris-HCl, 50 mM NaCl, *p*H 7.0, Tris = Tris (hydroxymethyl)aminomethane). Thermal DNA denaturation experiment was carried out in Buffer B (1.5 mM Na_2HPO_4, 0.5 mM NaH_2PO_4, 0.25 mM Na_2EDTA, EDTA = ethylene diaminetetraacetic acid, *p*H 7.0).

Viscosity measurements were carried out using an ubbelohde viscometer maintained at 29.0 ± 0.1 °C in a thermostatic bath. Flow time was measured with a digital stopwatch, and each sample was measured three times, and an average flow time was calculated. Data are presented as $(\eta/\eta_0)^{1/3}$ *versus* binding ratio[10], where η is the viscosity of DNA in the presence of complex and η_0 is the viscosity of CT-DNA alone.

The absorption titration experiments of Ru (II) complexes were performed at a fixed complex concentration (10 μM) until the absorbance did not change any more with increasing DNA. The complex–DNA solutions were allowed to incubate for 5 mins before the absorption spectra were recorded. The intrinsic binding constants K_b to DNA were determined using the Eqn. 1 (Ref. 11):

$$\frac{\varepsilon_a - \varepsilon_f}{\varepsilon_b - \varepsilon_f} = \frac{\sqrt{b - (b^2 - 2K_b^2 C_t [DNA]/s)}}{2KC_t} \quad \ldots (1a)$$

$$b = 1 + K_b C_t + K_b [DNA]/2s \quad \ldots (1b)$$

where [DNA] is the concentration of DNA in base pairs, the apparent absorption coefficients *a, f,* and *b* correspond to A_{obsd}/[Ru], the extinction coefficient for the free ruthenium complex, and the extinction coefficient for the ruthenium complex in the fully bound form, respectively. K_b is the equilibrium binding constant in M^{-1}, C_t is the total metal complex concentration, and *s* is the binding size.

Thermal denaturation studies were carried out with a Perkin–Elmer Lambda 35 spectrophotometer equipped with a Peltier temperature–controlling programmer (± 0.1 °C). The absorbance at 260 nm was continuously monitored for solutions of CT–DNA (100 M) in the absence and presence of the ruthenium (II) complex (10 M). The temperature of the solution was increased by 1 °C·min^{-1}.

Topoisomerase inhibition assay

DNA Topoisomerase I (Topo I) from calf thymus was purchased from MBI Fermentas, and no further purification was performed. One unit of the enzyme was defined as completely relaxes 1 g of negatively supercoiled pBR322 DNA in 30 min at 37 °C under the standard assay conditions. The reaction mixture (20 L) contained 35 mM Tris-HCl (*p*H 8.0), 72 mM KCl, 5 mM $MgCl_2$, 5 mM DTT, 2 mM spermidine, 0.1 mg/mL BSA, 0.1 g pBR322 DNA, 1 Unit Topo I, and Ru(II) complexes. The reaction mixtures were incubated at 37 °C for 30 min, and the reaction was terminated by addition of 4 L of 5 × stop solution consisting of 0.25% bromophenol blue, 4.5% SDS,

and 45% glycerol. The samples were electrophoresed through 1% agarose in TBE at 30 V for 8 hours. The gel was stained with 1 g/mL ethidium bromide and photographed under UV light. The concentrations of the inhibitor that prevented 50% of the supercoiled DNA from being converted into relaxed DNA (IC_{50} values) were calculated by the midpoint concentration for drug-induced DNA unwinding.

DNA Topoisomerase IIα (Topo II) from *E. coli* containing a clone of the human Topoisomerase II gene was purchased from GE Healthcare Bio-Sciences, and no further purification was performed. One unit of the enzyme was defined as completely relaxes 0.3 g of negatively supercoiled pBR322 plasmid DNA in 15 min at 30 °C under the standard assay conditions. The reaction mixture (20 L) contained 10 mM Tris-HCl (*p*H 7.9), 50 mM NaCl, 50 mM KCl, 5.0 mM $MgCl_2$, 0.1 mM Na_2H_2edta, 15 μg/mL BSA, 1.0 mM ATP, 0.1 μg pBR322 DNA, 2 Unit Topo II, and Ru (II) complexes. The reaction mixtures were incubated at 30 °C for 15 min. Reactions were stopped, processed, and subjected to gel electrophoresis as above.

DNA strand passage assay

The DNA strand passage activity of Topo I was determined by monitoring the ability of the enzyme to relax negatively supercoiled plasmid molecules in the absence of drug[12] or to supercoil relaxed plasmid substrates in the presence of intercalative agents[13]. DNA strand passage assays contained 0.3 μg pBR322 plasmid DNA (relaxed or supercoiled, as above) and Topo I (5 unit) in 40 μL of Topo I reaction buffer. Reactions were carried out in the absence of drug or in the presence of 40 μM Ru (II) complexes or ethidium bromide. Following a 5 min incubation of DNA with drug or water, Topo I was added, and reactions were incubated up to 15 min at 37 °C. Reactions were stopped, processed, and subjected to gel electrophoresis as above.

The Topo II DNA strand passage assay was examined in the presence of ethidium bromide and Ru (II) complexes. DNA strand passage assays contained 0.3 μg pBR322 plasmid DNA (relaxed or supercoiled, as above) and Topo II (10 unit) in 40 μL of Topo II reaction buffer. Reactions were carried out in the absence of drug or in the presence of 40 μM Ru (II) complexes or ethidium bromide. Following a 5 min incubation of DNA with drug or water, Topo II was added, and reactions were incubated up to 20 min at 30 °C. Reactions were stopped, processed, and subjected to gel electrophoresis as above.

Cell Lines and Cell Culture

Human cancer cell lines, including cervical carcinoma HeLa, hepatocellular carcinoma HepG2 and breast carcinoma MCF-7, were purchased from American Type Culture Collection (ATCC, Manassas, VA). The human hepatocellular carcinoma BEL-7402 was obtained from the Cell Bank (Cell Institute, Sinica Academica Shanghai, Shanghai, China). All cell lines were maintained in either RPMI-1640 or DMEM media supplemented with fetal bovine serum (10%), penicillin (100 units/mL) and streptomycin (50 units/mL) at 37 °C in CO_2 incubator (95% relative humidity, 5% CO_2).

MTT assay

In vitro cytotoxicity test were carried out by a standard MTT (3-(4,5-dimethylthiazole-2-yl)-2,5-diphenyltetrazolium bromide) colorimetric assay[14]. Cells were plated in 96-well microassay culture plates (1×10^4 cells per well) and grown overnight at 37 °C in a 5% CO_2 incubator. Test compounds were then added to the wells to achieve final concentrations ranging from 10^{-6} to 10^{-4} M. Control wells were prepared by addition of culture medium (100 μL). Wells containing culture medium without cells were used as blanks. The plates were incubated at 37 °C in a 5%CO_2 incubator for 48 h. Upon completion of the incubation, stock MTT dye solution (20 μL, 5 mg/mL) was added to each well. After 4 h incubation, buffer (100 μL) containing N,N-dimethylformamide (50%) and sodium dodecyl sulfate (20%) was added to solubilize the MTT formazan. The optical density of each well was then measured on a microplate spectrophotometer at a wavelength of 490 nm. The IC_{50} value was determined from plots of % viability against dose of compound added.

Flow Cytometric Analysis

HeLa cells in a density of 1×10^6 cells /mL were treated with IC_{50} concentration of Ru (II) complexes and incubated for 24, 48 and 72 h. Cells were trypsinized, harvested, and fixed with 1 mL of cold 70% ethanol in test tubes and incubated at 4 °C overnight. After incubation, the cells were centrifuged and washed in 1 mL phosphate-buffered saline (PBS) and resuspended in 0.4 mL PBS. To a 0.5 mL cell

sample, 50 μL RNase (type I-A, Sigma) (1 mg/mL in PBS), was added and incubated for 30 min at 37 °C followed, after gentle mixing, by 50 μL propidium iodide (Sigma, 500 μg/mL in PBS) solution. The mixed cells were incubated in the dark at RT for 15 min and kept at 4 °C in the dark until measured. The cell cycle distribution was analyzed with FACSCanto II (BD Biosciences, USA). The data were acquired and analyzed with BD FACSDiva software v6.0.

Annexin V-FITC/PI Double Staining

After incubation with different concentrations (25, 50, 100 and 200 μmol/L) of Ru(II) complexes for 24 hours, 1×10^6 HeLa cells were trypsinized, washed twice with ice-cold PBS and then re-suspended in 100 μL binding buffer (50 mmol/L HEPES/NaOH, *p*H 7.4, 700 mmol/L NaCl, 12.5 mmol/L $CaCl_2$) containing 5 μL of Annexin V-FITC/PI Double Staining stock (Invitrogen, Paisley, UK) and 1 μL of 1 mg/mL PI (Sigma, USA). After incubation for 15 minutes at RT in a light-protected area, Another 400 μL binding buffer was added and the specimens were quantified by flow cytometry on a FACSCanto II (BD Biosciences, USA).

Acridine Orange/Ethidium Bromide (AO/EB) Staining

Apoptosis studies were performed with a staining method utilizing acridine orange (AO) and ethidium bromide (EB)[15]. According to the difference in membrane integrity between necrotic and apoptosis, AO can pass through cell membrane, but EB can not. Under fluorescence microscope, live cells appear green. Necrotic cells stain red but have a nuclear morphology resembling that of viable cells. Apoptosis cells appear green, and morphological changes such as cell blebbing and formation of apoptotic bodies will be observed. A monolayer of HeLa cells was incubated in the absence or presence of Ru(II) complexes at concentration of 125 μM at 37 °C and 5% CO_2 for 24 h and 48 h. After 24 h or 48 h, cells were stained with AO/EB solution (100 μg/mL AO, 100 μg/mL EB). Samples were observed under an inverted fluorescence microscope (Zeiss Axio Observer D1).

Statistics Analysis

All the data are expressed as mean ± SD. Differences between two groups were analyzed by two-tailed Student's t test. One-way analysis of variance (ANOVA) was used in multiple group comparisons. These analyses were carried out by SPSS 12.0. Difference with $P < 0.05$ (*) was considered statistically significant.

Results and Discussion

Synthises and characterization

The synthesis route was shown in Scheme S1. Similar to that described by Hanant[16] and Balzani[17] the ligand adtpy was prepared by condensation reaction of 2-Acetylpyridine and 2-formyl-9,10-anthraquinone in the presence of EtOH, KOH pellets and aq NH_3. Reactions of 1 equiv of adtpy with $Ru(tpy)Cl_3$ or $Ru(dtp)Cl_3$ in glycol in the presence of 1mL triethylamine at 120 °C for 8 h, followed by metathesis with $NaClO_4$, afforded the heteroleptic ruthenium complexes $[Ru(L)(adtpy)][ClO_4]_2$ (L = tpy, dtp). The ruthenium complexes were purified by column chromatography [alumina, acetonitrile-toluene (5:1 v/v) as eluent] and characterized by ^{1}H NMR, ES MS and elemental analyses. In the ES-MS spectra for thecomplexes, only the signals $[M-2ClO_4]^{2+}$ and $[M-2ClO_4]^{2+}$ were observed. The measured molecular weights were consistent with expected values.Due to the shielding influences of the adjacent adtpy and tpy,, the chemical shifts of hydrogen atoms of Ligand neighbouring coordination metal center were moved to highfield. Part of the protons were the lowfield mobility caused by inductive effect. The absorption spectra of $[Ru(tpy)(adtpy)][ClO_4]_2$ and $[Ru(dtp)(adtpy)][ClO_4]_2$ are characterized by intense π-π* ligand transitions in the UV and metal-to–ligand charge transfer (MLCT) transition in the visible region. The broad MLCT absorption band appears at 489 nm and 482nm for both complexes. The peaks at 307 and 324 nm are assigned to the internal π-π* transition of the ligands. $[Ru(tpy)(adtpy)][ClO_4]_2$ and $[Ru(dtp)(adtpy)][ClO_4]_2$ display no luminescence in both organic solvents and in Tris–HCl buffer. This can be attributed to the intramolecular photoinduced electron transfer (PET) from the MLCT state of Ru(II) complex to the appended quinone accepter. Similar cases had been observed in $[Ru(phen)_2(qdppz)]^{2+}$ (Ref. 18) and $[Ru(bpy)_2(bpy\text{-}BQ)]^{2+}$ (where bpy-BQ is a quinone appended bipyridine ligand)[19].

DNA binding studies

Viscosity measurements were carried out to clarify the nature of the interaction between complexes and DNA. Intercalators generally increase the

hydrodynamic length of DNA, while groove binders do not lengthen the DNA molecules[20]. Viscosity measurement can sensitively detect the lengthening and unwinding of the DNA helix induced by the binding of intercalators[21], and thus provides evidence of intercalation of small DNA-binding molecules. The affect of complexes **1**, **2** and ethidium bromide (EB) on the viscosity of rod–like DNA is shown in Fig. 1. As expected, the known DNA intercalator EB increase the relative specific viscosity for the lengthening of the DNA double helix resulting from intercalation. On increasing the amounts of complexes **1** and **2**, the relative viscosity of DNA increasing steadily, which are similar to the behavior of EB. The increased degree of viscosity, which may depend on its affinity to DNA, follow the order of EB > $[Ru(tpy)(adtpy)]^{2+}$ > $[Ru(dtp)(adtpy)]^{2+}$. These results suggest that both complexes **1** and **2** bind to DNA *via* the intercalating mode. The difference in binding strength of complex **1** and **2** are due to the ancillary ligand.

The absorption spectra of complexes **1** and **2** in the absence and presence of CT-DNA are given in Fig. 2, which unambiguously reveals that intense hypochromism and bathochromism in the UV-visible region occur. As the concentration of DNA is increased, the hypochromism in the MLCT band decreases and obvious red shift of the complexes is observed. For complex **1**, the hypochromism at 489 nm reached 22.04%, with a red shift of 6 nm at a [DNA]/[Ru] ratio of 20. For complex **2**, under the same experimental condition, the hypochromism at 482nm was found for 17.82%, with a red shift of 7 nm at a [DNA]/[Ru] ratio of 20. From the decay of the absorbance of Ru (II) complexes monitored at the MLCT band (at 489 nm for complex **1**, and at 482 nm for complex **2**) upon addition CT-DNA, an intrinsic binding constant K of $(1.33 \pm 0.36) \times 10^6\ M^{-1}$ (s = 0.25 ± 0.018) and $(1.12 \pm 0.24) \times 10^6\ M^{-1}$ (s = 0.33 ± 0.020) was determined with the McGhee-Von Hippel (MVH) model[11], respectively. The result is comparable to those of $[Ru(bpy)_2(pip)]^{2+}$[22], $[Ru(phen)_2(ppd)]^{2+}$ (ppd = pteridino[7,6-*f*][1,10]phenanthroline-1,13(10H,12H)-dione)[23], $[Ru(bpy)_2(dppz)]^{2+}$ [24], $[Ru(phen)_2dppz]^{2+}$ [25] and the known DNA intercalator EB ($1.4 \times 10^6\ M^{-1}$) [26].

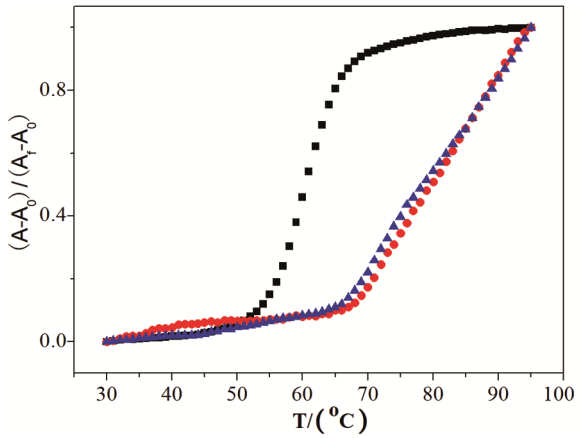

Fig. 1 — Effect of increasing amounts of ethidium bromide (■), complex **1** (▲) and complex **2** (▼) on the relative viscosity of calf thymus DNA at 29(±0.1)°C. The total concentration of DNA is 0.25 mM.

Thermal behaviors of DNA in the presence of complexes can further give insight into DNA conformational changes when temperature is raised, and offer information about the interaction strength of complexes with DNA. It is well known that when the temperature in the solution increases, the double-stranded DNA gradually dissociates to single strands[27], and generates a hypochromic effect on the

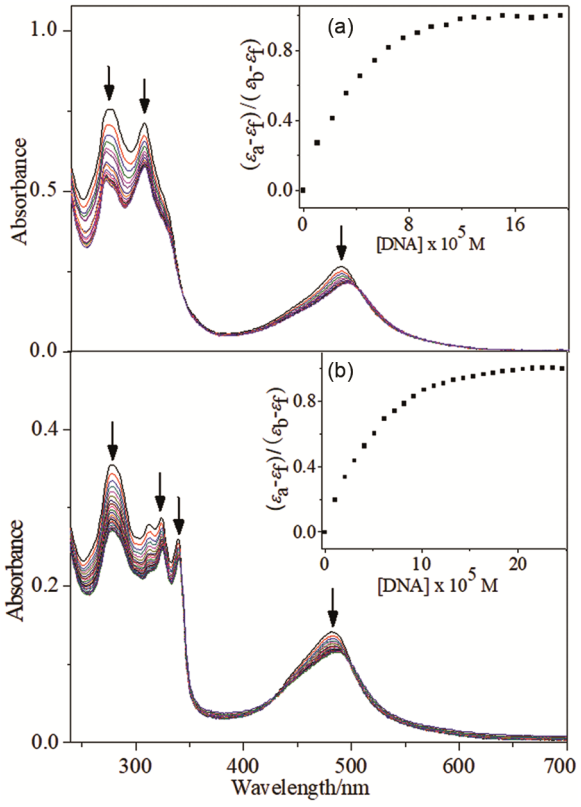

Fig. 2 — Absorption spectra of complexes **1** (a) and **2** (b) in Tris-HCl buffer upon addition of CT DNA ([Ru] = 10^5 M, [DNA] = 0-200 μM). Arrows indicate the change in absorbance upon increasing the DNA concentration. Insert: Plot of $(\varepsilon_a - \varepsilon_f)/(\varepsilon_b - \varepsilon_f)$ *vs.* [DNA] for the titration of DNA to complexes **1** and **2**.

absorption spectra of DNA bases (λ_{max} = 260 nm). To identify this transition process, the melting temperature, T_m, which is defined as the temperature where half of the total base pairs is unbonded, is usually introduced. Generally, the melting temperature increases when metal complexes bind to DNA by intercalation, as intercalation of the complexes into DNA base pairs causes stabilization of base stacking and hence raises the melting temperature of the double-stranded DNA, DNA melting experiments are useful in establishing the extent of intercalation[28]. According to the previous reports[29,30], the intercalation of natural or synthesized organic and metallointercalators generally results in a considerable increase of T_m. The melting curves of CT-DNA in the absence and presence of complexes **1** and **2** are presented in Fig. 3. Here, the thermal denaturation experiment carried out for DNA in the absence of the Ru (II) complexes revealed a T_m of 60.5 ± 0.2 °C under our experimental conditions. The observed melting temperature in the presence of complexes were 82.4 ± 0.2 °C and 81.2 ± 0.2 °C for complexes **1** and **2**, respectively, at a concentration ratio [Ru]/[DNA] = 1:10. The large increases in T_m of DNA with two Ru (II) complexes (The ΔT_m is 21.9 and 20.7 °C for **1** and **2**, are comparable to that observed for classical intercalators[29,30]. As we know, The melting points were increased by 13, 18, 16 for EB, $[Ru(phen)_3]^{2+}$ and Δ-$[Ru(phen)_2(dppz)]^{2+}$, respectively[31]. The DNA intrinsic binding constant at

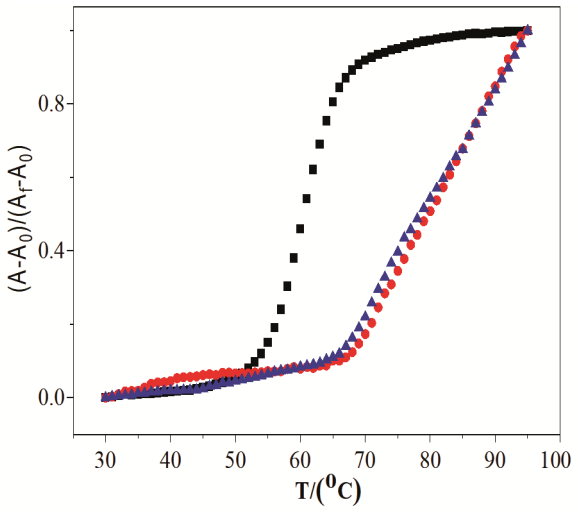

Fig. 3 — Effect of increasing amounts of ethidium bromide (■), complex **1** (▲) and complex **2** (▼) on the relative viscosity of calf thymus DNA at 29(±0.1)°C. The total concentration of DNA is 0.25 mM.

melting temperature can be obtained from the McGhee equation (*Eqn*. 4)[32].

$$\frac{1}{T_m^0} - \frac{1}{T_m} = \left(\frac{R}{\Delta H_m}\right) \ln(1 + KL)^{1/n} \quad \ldots (4)$$

where T_m° is the melting temperature of CT–DNA alone, T_m is the melting temperature in the presence of the ruthenium (II) complex, ΔH_m is the enthalpy of DNA (per base pair), R is the gas constant, K is the DNA binding constant at T_m, L is the free complex concentration (approximated at the T_m by the total complex concentration), and n is the size of the binding site.

For the CT-DNA used in these studies, under identical solution conditions, a melting enthalpy of 6.9 kcal·mol^{-1} was determined by differential scanning calorimetry [10]. On the basis of the absorption spectra titration experiment and neighbor exclusion principle, the values of n for both complexes were assumed to be 2.0 bp. The values of K are 1.33 × 10^6 M^{-1} and 1.12 × 10^6 M^{-1} for complexes **1** and **2**, respectively. The K values indicate that the complexes still display binding affinity at the melting point of DNA. The standard enthalpy, standard entropy and the standard free energy change of the binding of complexes **1** and **2** to CT-DNA were determined by van't Hoff's[33].

$$\ln\left(\frac{K_1}{K_2}\right) = \frac{\Delta H^0}{R}\left(\frac{T_1 - T_2}{T_1 T_2}\right) \quad \ldots (5)$$

$$\Delta G^0 = -RT \ln K \quad \ldots (6)$$

$$\Delta G^0 = \Delta H^0 - T\Delta S^0 \quad \ldots (7)$$

where K_1 and K_2 are the DNA-binding constants of the metal complex at temperatures T_1 and T_2, respectively, and ΔH°, ΔG°, and ΔS° are the standard enthalpy, standard free energy, and standard entropy change of the metal complex binding to DNA, respectively. The values of ΔH°, ΔG° and ΔS° at 25 °C were found to be –51.3 kJ·mol^{-1}, –34.9 kJ·mol^{-1} and –55.0 J·mol^{-1}·K^{-1} for complex **1** and –50.6 kJ·mol^{-1}, –34.5 kJ·mol^{-1} and –54.0 J·mol^{-1}·K^{-1} for complex **2**. The negative binding free energy implies that the sum of the free energies of free complexes and DNA is higher than that of the adduct, and the binding of the Ru (II) complexes to CT-DNA is energically highly favorable at 298 K, and the binding reaction was driven enthalpically. The negative entropy values indicate that the degree of freedom of the Ru (II) complexes is

decreased after the binding, and that the DNA conformational freedom is also reduced upon complex-DNA binding. Upon intercalation at the unwound site, there is a substantial structural overlap between the base pairs and the intercalator. The intercalator becomes rigidly held and oriented with the planar moiety perpendicular to the helical axis. Intercalation produces an unwinding, and stiffening of the DNA helix. These changes are a consequence of the untwisting of the base pairs and helical backbone needed to accommodate the intercalator.

Topoisomerase inhibition

The results of Topo I inhibition assay by different concentrations of complexes **1** and **2** are shown in Fig. 4. Both complexes inhibited the ability of Topo I to relax negatively supercoiled plasmid DNA (IC_{50} is ~10 μM for complex **1** and ~9 μM for complex **2**). These findings imply that both complexes may block the DNA strand passage event of the enzyme, and serve as catalytic inhibitors of Topo I. However, as DNA intercalators, the complexes can directly alter the topological state of the negatively supercoiled DNA substrate by inducing constrained negative and unconstrained positive superhelical twists in plasmid DNA. Since Topo I removes only the unconstrained positive supercoils, the negatively supercoiled DNA product would be identical to the topological state of the original plasmid substrate. In this case, the complexes will also appear to inhibit enzyme catalysis.

As DNA intercalators, the complexes can directly alter the topological state of the negatively supercoiled DNA substrate by inducing constrained negative and unconstrained positive superhelical twists in plasmid DNA. Since Topo I removes only the unconstrained positive supercoils, the negatively supercoiled DNA product would be identical to the topological state of the original plasmid substrate. In this case, the complexes will also appear to inhibit enzyme catalysis. To determine whether the complexes interfere with the DNA relaxation reaction by inhibiting Topo I catalysis or by altering the apparent topological state of DNA, the DNA strand passage assay was performed[34]. The effects of the complexes on enzyme-catalyzed DNA strand passage were assessed by comparing the rate of relaxation of negatively supercoiled plasmid in the absence of drug to the rate of supercoiling of relaxed plasmid in the presence of EB. As shown in Fig. 5, the rate of Topo I-catalyzed DNA supercoiling in the presence of the Ru (II) complexes were lower than the rate of EB, which was identical to the rate of Topo I-catalyzed DNA relaxation in the absence of drug. These findings suggest that complexes **1** and **2** are catalytic inhibitors of topoisomerase I.

The results of concentration-depended Topo II inhibition assay of complexes **1** and **2** are shown in Fig. 6. Two Ru (II) complexes inhibited the activity of Topo II at a low concentration (IC_{50} is ~6 μM for complex **1** and ~7 μM for complex **2**), comparing with some classical topoisomerase inhibitors (Table 1). Similar to that described above for Topo I, DNA strand passage assay was also used to distinguish the effects of Ru (II) complexes on Topo II function from their effects on DNA topology. As shown in Fig. 7, the religation rate of the relaxed plasmid in the presence of Ru (II) complexes are lower than that of EB. These findings suggest that complexes **1** and **2** are a catalytic inhibitor (or poison) of human Topoisomerase IIα.

Inhibition of Cell Proliferation and Cytotoxicity

The *in vitro* cytotoxic activities of the Ru (II) complexes were evaluated against HeLa, MCF-7, HepG2 and BEL-7402 tumor cell lines. Table 2 shows the IC_{50} values of $[Ru(tpy)(adtpy)]^{2+}$,

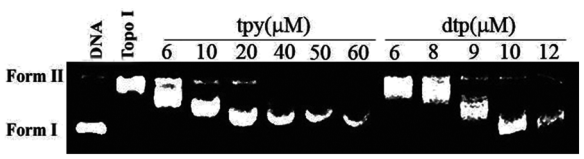

Fig. 4 — Effects of different concentrations of complexes **1** and **2** on the activity of DNA topoisomerase I (Topo I).

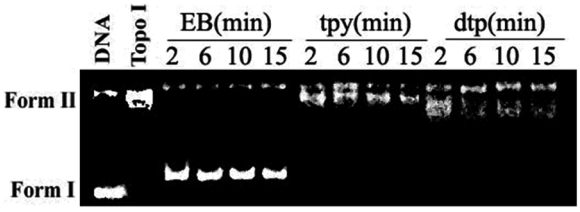

Fig. 5 — The time dependence of Topo I DNA strand passage assays in the presence of ethidium bromide (EB) and complexes **1** and **2**.

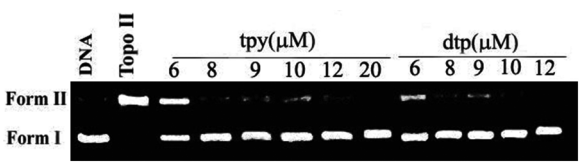

Fig. 6 — Effects of different concentrations of complexes **1** and **2** on the activity of DNA topoisomerase IIα (Topo II)

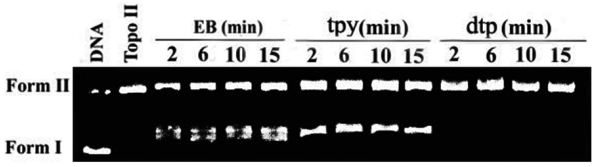

Fig. 7 — The time dependence of Topo II DNA strand passage assays in the presence of ethidium bromide (EB) and complexes **1** and **2**.

Table 1 — Inhibitory effects of $[Ru(tpy)(adtpy)]^{2+}$and $[Ru(dtp)(adtpy)]^{2+}$ on topoisomerases I and II activities

Drug	Inhibitory activity (IC_{50})		Ref.
	Topoisomerase I	Topoisomerase II	
Camptothecin	17	> 100	44
Doxorubicin	> 100	1	44
Novobiocin	> 100	32	44
Etoposide	> 1000	35	45
Hoechst 33258	30	35	46
Topostatin	17	4	44
Δ-$[Ru(bpy)_2(uip)]^{2+}$	~ 40	3	47a
Λ-$[Ru(bpy)_2(uip)]^{2+}$	~ 40	5	47a
$[Ru(bpy)_2(appo)]^{2+}$	~ 25	< 1	47b
$[Ru(tpy)(adtpy)]^{2+}$	10	6	This work
$[Ru(dtp)(adtpy)]^{2+}$	9	7	This work

Table 2 — IC_{50} values of $[Ru(tpy)(adtpy)]^{2+}$and $[Ru(dtp)(adtpy)]^{2+}$ towards different tumor cell lines

Complex	IC_{50} (mM)			
	HeLa	BEL-7402	MCF-7	Hep-G2
$[Ru(tpy)(adtpy)]^{2+}$	0.125	0.396	0.066	0.17
$[Ru(dtp)(adtpy)]^{2+}$	0.141	0.492	0.075	0.219
5-Fluorouracil	1.23	2.43	1.60	0..87
Cisplatin	0.016	0.026	0.024	0.027

$[Ru(dtp)(adtpy)]^{2+}$, 5-Fluorouracil and cisplatin by MTT assay after a 48 h treatment. The tested cancer cells, especially the MCF-7 cells, were susceptible to the complexes. Both the complexes demonstrated higher *in vitro* cytotoxicity against selected tumor cell lines than 5-Fluorouracil, a widely used clinical antitumor drug, but relative lower cytotoxicity than cisplatin. The two complexes displayed small difference in the antitumor activity against the tested tumor cells. The $[Ru(tpy)(adtpy)]^{2+}$ is more active against the tumor cell lines than $[Ru(dtp)(adtpy)]^{2+}$. The small difference in cytotoxicity of the two complexes may imply the cytotoxicity is relative to the topoisomerase inhibition activity, because the complexes show a little difference in the DNA binding.

Most commonly used conventional *in vitro* assays for cell viability are end-point assays which eventually also require lysis of cells. Recently real-time monitoring of target cell status based on electrical impedance measurements has been introduced as a continuous and nonradioactive method for assessing cellular cytotoxicity *in vitro*[35]. 10,000 HeLa cells/well concentration in the real-time cell growth and proliferation assay was used to examine the toxic effects elicited by $[Ru(tpy)(adtpy)]^{2+}$ and $[Ru(dtp)(adtpy)]^{2+}$, respectively. As shown in Fig. 8, kinetic profiles provided by the xCELLigence System indicate that the rate and dynamics of cytotoxicity were similarly between the complexes. Interestingly, cell killing kinetics were shown to be concentration-dependent. Cells treated at high doses of Ru (II) complexes (200 and 150 μM) can rapidly abolished continuous cellular proliferation, indicating that cells undergo irreversible senescence. Whereas, cells treated at at low doses of Ru (II) complexes (12.5 μM) seem to overcome the cellular damage, reaching control Cell Index levels with a short delay. This is most likely due to a DNA damage-mediated cell cycle arrest, which is eventually overcome after the damage is repaired by the cellular DNA repair machinery. In addition, the complexes treatment in the two kinds of cells were found to cause a rapid onset and progression of cell death, making it difficult to identify the ideal time point for functional endpoint assays. The impedance-based CI values clearly revealed cytotoxic effects in real-time, allowing pinpointing when to perform biochemical endpoint assays in downstream applications addressing questions in proteomics and genomics.

Cell Cycle Analysis

To investigate the mechanism of cell division and cell death induced by $[Ru(tpy)(adtpy)]^{2+}$ and $[Ru(dtp)(adtpy)]^{2+}$ on HeLa cells, the fluorescence-activated cell sorting (FACS) analysis of the DNA content was performed. The cells were treated with the complexes, the cell cycle progression was analyzed at different concentrations of Ru(II) complexes for 24 h (Fig. 9). In the control experiments, 0.63% of the cells were found to be populated at sub-G_1 (apoptotic) phase, and also, higher percentages of cells were populated at the G_0/G_1 phase (50.18%) and lower percentages of cells were populated at the S phase (35.59%) and G_2/M phases (14.23%). It is well known that in this analysis, the cells in the G_0/G_1 phase have

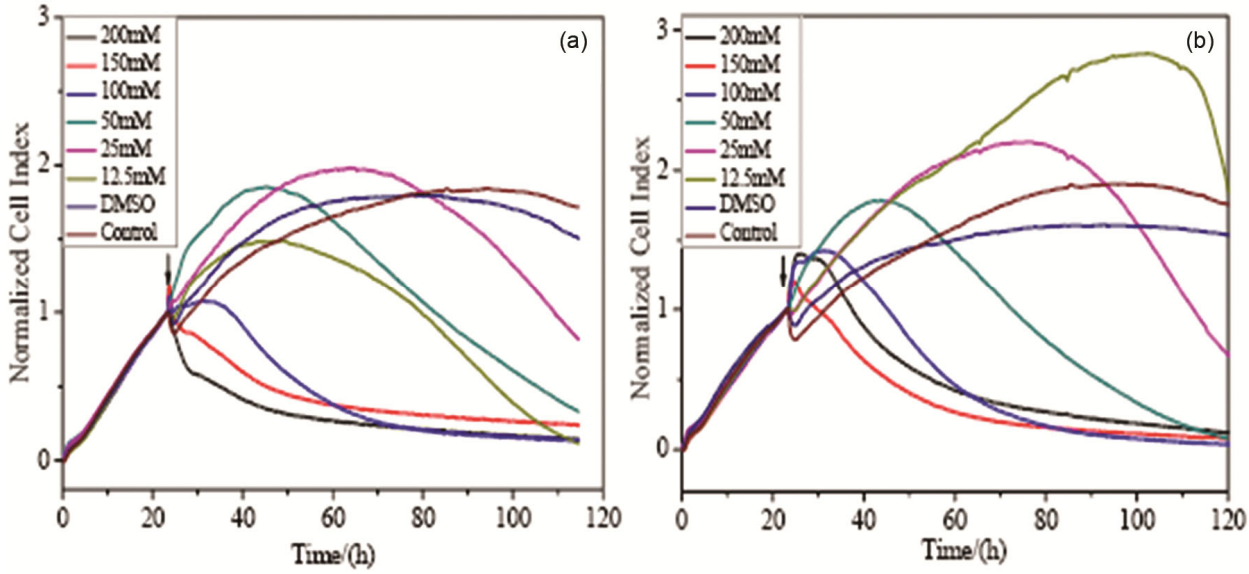

Fig. 8 — Kinetics of cytotoxicity responses for Ru (II) complexes in cellsmonitored by thexCELLigence system. (a) $[Ru(tpy)(adtpy)]^{2+}$ in HeLa, (b) $[Ru(dtp)(adtpy)]^{2+}$ in HeLa. 10,000 cells/well were plated in16-well strips for the RT-CES cytotoxicity assay. ↓, the time of compound addition.

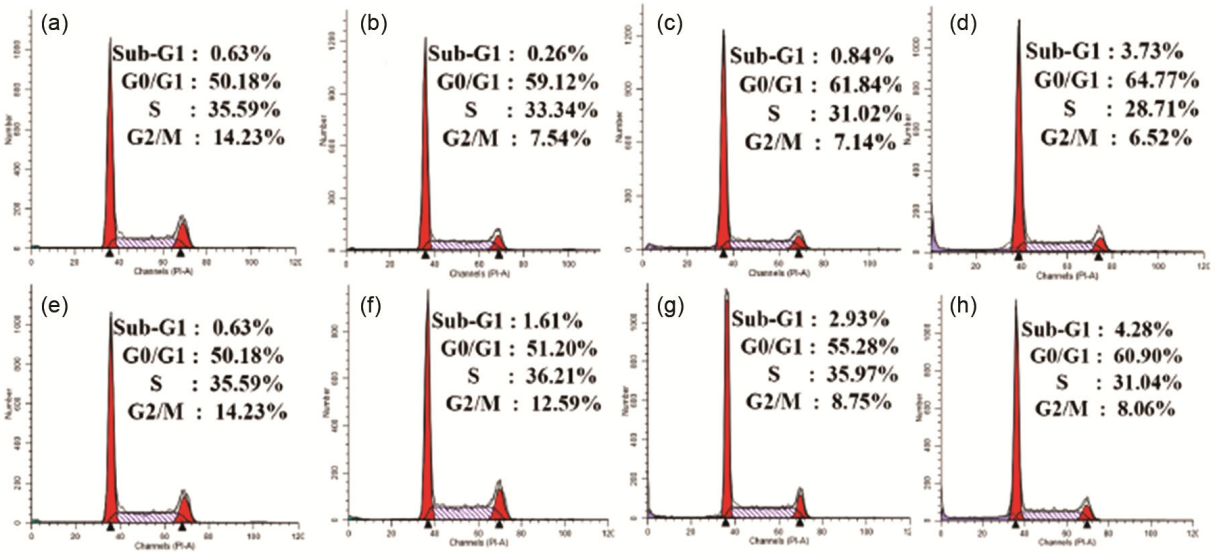

Fig. 9 — $[Ru(tpy)(adtpy)]^{2+}$ and $[Ru(dtp)(adtpy)]^{2+}$ induced apoptotic cell death as examined by flow cytometric analysis. Cells were treated with different concentrations of Ru(II) complexes for 24 h. (a) and (e)Control, $[Ru(tpy)(adtpy)]^{2+}$ (25μM), (c) $[Ru(tpy)(adtpy)]^{2+}$ (50μM), (d) $[Ru(tpy)(adtpy)]^{2+}$ (100μM), (f) $[Ru(dtp)(adtpy)]^{2+}$ (25μM), (g) $[Ru(dtp)(adtpy)]^{2+}$ (50μM), (h) $[Ru(dtp)(adtpy)]^{2+}$ (100μM).

unreplicated diploid (2n) DNA content, whereas the G_2/M phase has replicated ploid (4n) DNA. Also, hypodiploidy (< 2n) DNA content at the sub-G1 phase and replication in the S phase are observable. Upon exposure of the cells to $[Ru(tpy)(adtpy)]^{2+}$, the accumulation of cells increased in the sub-G_1 phase from 0.63 (control) to 3.73% ([Ru] = 100 μM), and G_0/G_1 phase from 50.18 (control) to 64.77% ([Ru] = 100 μM), and thus the percentage of cells accumulated at these phases increased with the concentrations of Ru (II) complexes. Also, the percentages of cells decreased in the remaining phases of the cell cycle (G_2/M, 14.23 to 6.52%; S, 35.59 to 28.71%) with the increment of Ru (II) complexes. Compared with the untreated control, $[Ru(tpy)(adtpy)]^{2+}$ disturb cell cycle strongly and induce an obvious arrest in sub-G_1 and G_0/G_1 phases. Similar cases have also been observed for

$[Ru(dtp)(adtpy)]^{2+}$. All of these observations reveal that the major mode of cell death induced by the two complexes is apoptosis because the accumulation of hypodiploid cells in the sub-G_1 phase is considered to be a marker for apoptotic cell death [21,22]. Several intracellular cascades such as activation of caspases, disruption of normal mitochondrial function, or both would be involved in the road map toward the final destination, that is, the apoptotic cell death[36]. Similar results have also been observed for the two complexes (50 μM) induced apoptotic cell death with different time for 24 h, 48 h, and 72 h. as examined by flow cytometric analysis (Fig. 10).

Apoptosis Induction

Cell death can be divided into two types: necrosis (accidental cell death) and apoptosis (programmed cell death)[37]. Necrotic cells undergo cell lysis and lose their membrane integrity, and severe inflammation is induced[38]. Apoptotic cells, however, are transformed into small membrane-bound vesicles (apoptotic bodies) which are engulfed *in vivo* by macrophages, and no inflammatory response is found[39]. Harmless removal of cells (cancer cells, for example) is one consideration in chemotherapy[40]. Therefore, induction of apoptosis is one of the considerations in the drug development, most of the cytotoxic anticancers drugs in current use have been shown to induce apoptosis in susceptible cells[41].

The type of cell death induced by Δ-$[Ru(bpy)_2(ipad)]^{2+}$ and Λ-$[Ru(bpy)_2(ipad)]^{2+}$ was investigated by the apoptosis assays-acridine orange/ethidium bromide (AO/EB) staining[7]. AO is a vital dye and can stain both live and dead cells. EB stains only cells that have lost their membrane integrity. Under the fluorescence microscope, live

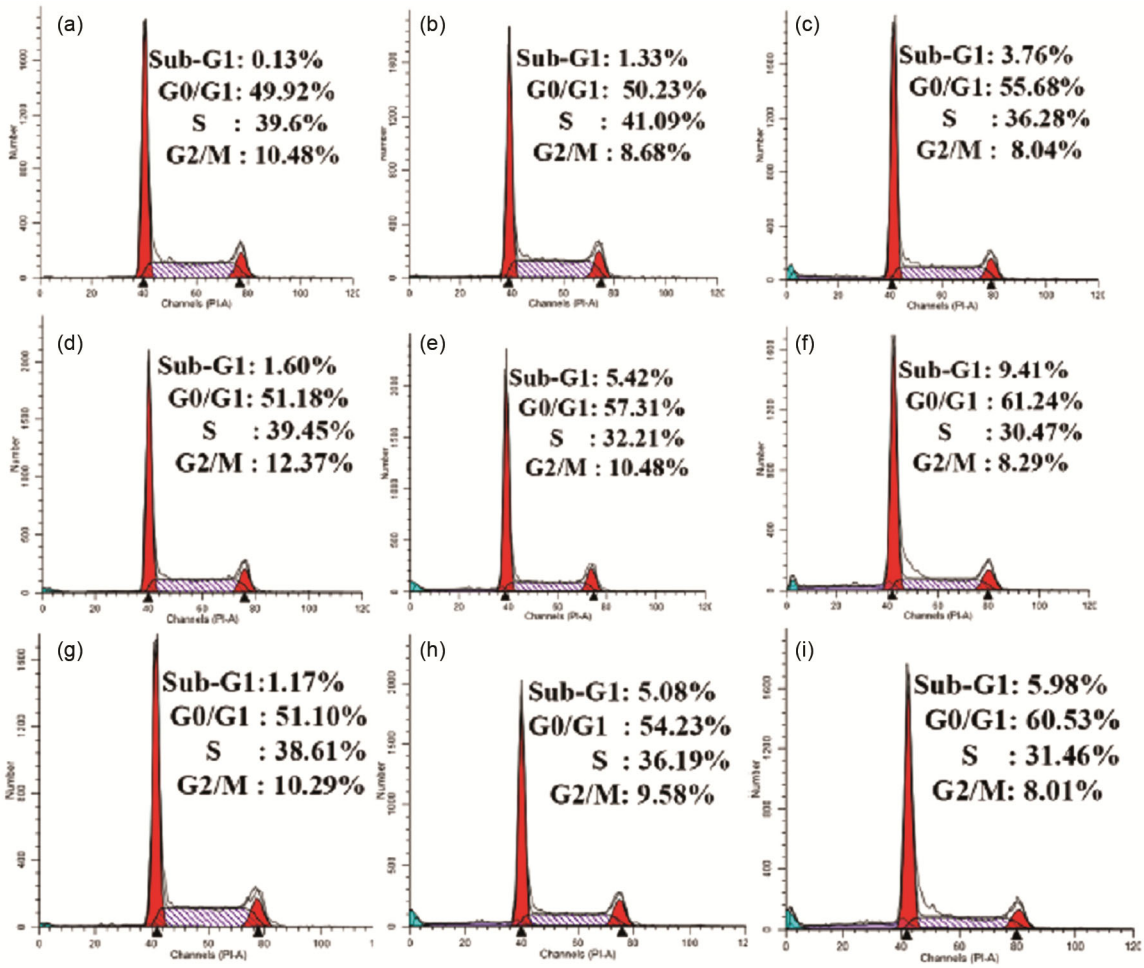

Fig. 10 — $[Ru(tpy)(adtpy)]^{2+}$ and $[Ru(dtp)(adtpy)]^{2+}$ induced apoptotic cell death as examined by flow cytometric analysis. Cells were treated with different time for Control (a) 24h, (b) 48h, (c) 72h. and of 50μM $[Ru(tpy)(adtpy)]^{2+}$(d) 24h, (e) 48h, (f) 72h. and of 50μM $[Ru(dtp)(adtpy)]^{2+}$(g) 24h, (h) 48h, (i) 72h.

cells appear green. Necrotic cells stain red, but have a nuclear morphology resembling that of viable cells. Apoptotic cells appear green and morphological changes such as cell blebbing and formation of apoptotic bodies will be observed. Microphotographs of AO/EB stained HeLa, which were pretreated for 24 h and 48 h with Ru (II) complexes, showed that $[Ru(tpy)(adtpy)]^{2+}$ and $[Ru(dtp)(adtpy)]^{2+}$ induced apoptosis (Fig. 11). Some of apoptotic cells have been even detected in the secondary necrosis. As shown, two complexes can induce apoptosis seen as condensation of nuclei in HeLa cells after 24 h. On treatment of the cells with the two enantiomers for a longer time of 48 h, the clear morphological change was observed for the necrotic cells staining uniformly orange. The results suggested that $[Ru(tpy)(adtpy)]^{2+}$ and $[Ru(dtp)(adtpy)]^{2+}$ caused predominantly apoptosis of HeLa cells.

Externalization of phosphatidylserine in the outer surface of the plasma membrane is a known hallmark of apoptosis or cell necrosis. The difference between these two forms of cell death is that during the early stages of apoptosis, the cell membrane remains intact, whereas at the very moment that necrosis occurs, the cell membrane looses its integrity and becomes leaky[42]. Therefore, the measurement of annexin V binding to the cell surface as indicative for apoptosis has to be performed in conjunction with a dye exclusion test to establish integrity of the cell membrane[42]. In combination with the membrane-impermeable DNA stain propidium iodide (PI), with a flow cytometer, one can distinguish at least three different cell types during apoptosis: viable cells (annexin V- and PI-negative), early apoptotic cells (annexin V-positive but PI-negative), and necrotic or late apoptotic cells (annexin V- and PI-positive)[42,43]. In a search of the nature of cell death induced by Ru (II) complexes, we performed double staining using Alexa Fluor® 488 annexin V and PI and analyzed by flow cytometry. The results showed a concentration dependent increase in annexin V binding in HeLa cells. Moreover, cells became annexin V^+ at a concentration that was much lower than their IC_{50} values. As shown in Fig. 12. In a concentration as low as 25 μM, annexin V^+ cells were detected and in 50 μM, 3.9% HeLa cells were in early apoptotic phase whereas 12.2% cells were in late apoptotic phase in 24 h. However, at 200 μM, a total of 62.3% (early apoptotic + late apoptotic) cells were undergoing apoptosis whereas untreated cells remained 100% viable. The cell death induced by $[Ru(tpy)(adtpy)]^{2+}$ follows such a pathway, *i.e.* from the lower left quadrant (Annexin V^-/PI^-) to the lower right quadrant (Annexin V^+/PI^-) and then to the upper right quadrant (Annexin V^+/PI^+). This suggested that induced cell death mainly through apoptosis. Similar cases have also been observed for $[Ru(dtp)(adtpy)]^{2+}$.

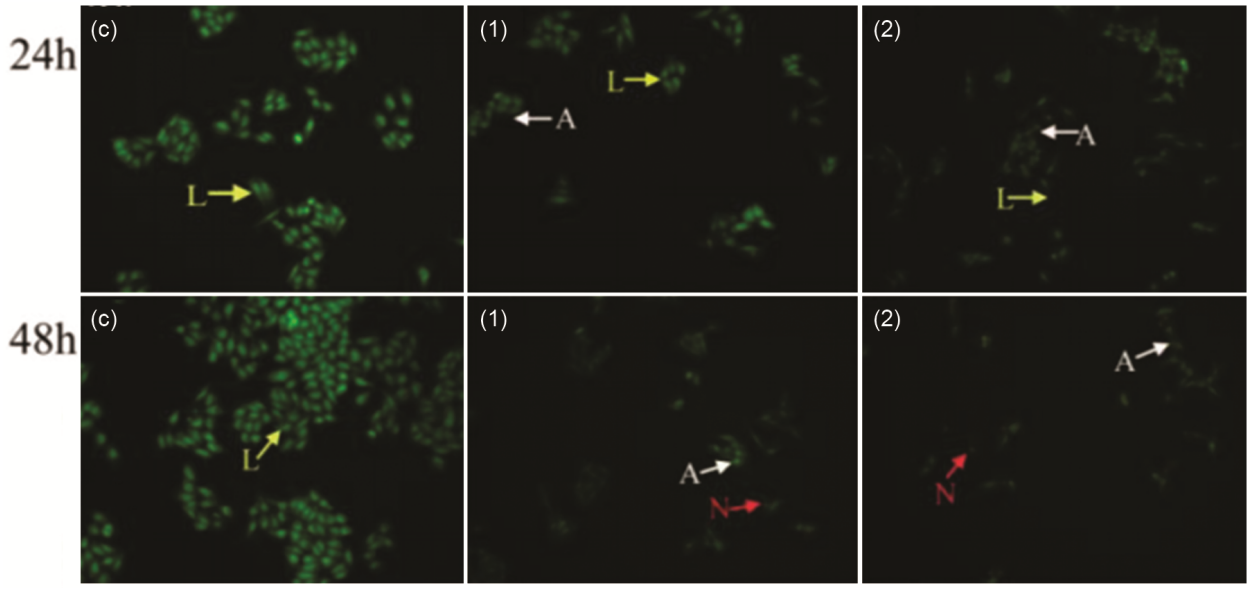

Fig. 11 — Hale cells were stained by AO/EB and observed under fluorescence microscope: (C) HeLa cell without treatment; (1) in the presence of complex **1** (50 μM); (2) in the presence of complex **2** (50μM); incubated at 37 °C and 5% CO_2 for 24 h and 48 h. Arrows point to the cells representing certain cell viable status: L, is the live cells; A, the apoptotic cells; and N, the necrotic cells.

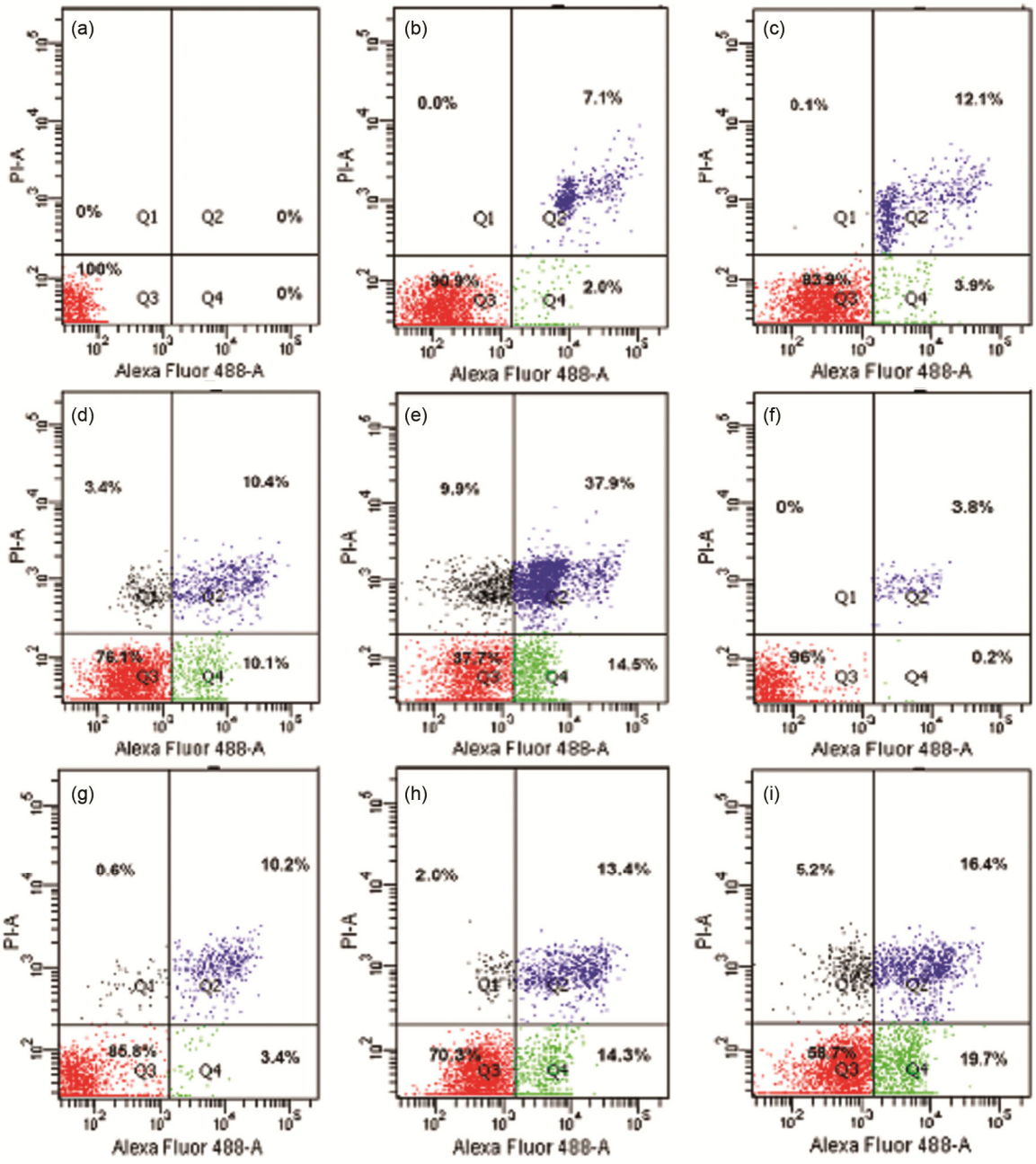

Fig. 12 — Ru (II) complexes and induced apoptotic cell death as examined by Annexin V-FITC/PIassay. HeLa cells were treated with different concentrations of Ru(II) complexes for 24 h. (a) Control, (b) $[Ru(tpy)(adtpy)]^{2+}$ (25μM), (c) $[Ru(tpy)(adtpy)]^{2+}$ (50μM), (d) $[Ru(tpy)(adtpy)]^{2+}$ (100μM), (e) $[Ru(tpy)(adtpy)]^{2+}$ (200μM), (f) $[Ru(dtp)(adtpy)]^{2+}$ (25μM), (g) $[Ru(dtp)(adtpy)]^{2+}$(50μM), (h) $[Ru(dtp)(adtpy)]^{2+}$ (100μM), (i) $[Ru(dtp)(adtpy)]^{2+}$ (200μM), The percentage of cells states arecited in each quadrant (Q2: late apoptotic or necrotic cells, Q3: viable cells, Q4: early apoptotic cells).

Conclusions

In summary, two ruthenium (II) complexes $[Ru(tpy)(adtpy)]^{2+}$ (**1**) and $[Ru(dtp)(adtpy)]^{2+}$ (**2**) have been synthesized and characterized. The DNA-binding, topoisomerase inhibition, cytotoxicity of the complexes and apoptosis assay were studied. As we expect, an intercalative binding mode between the Ru(II) complexes and DNA has been supported by various spectral experiments and hydrodynamic measurements. $[Ru(tpy)(adtpy)]^{2+}$ and $[Ru(dtp)(adtpy)]^{2+}$ have been found to possess an obviously greater affinity with DNA. Topoisomerase

inhibition and DNA strand passage assay confirm that two Ru (II) complexes act as efficient dual inhibitors of topoisomerases I and II. Moreover, both complexes show high antitumor activity to HeLa, MCF-7, HepG2 and BEL-7402 tumor cells. Apoptosis assay and cell circle analysis show that two Ru (II) complexes are capable of entering the cell and inducing cell apoptosis.

Supplementary Information

Supplementary information is available in the website http://nopr.niscpr.res.in/handle/123456789/58776.

Acknowledgements

This work was supported by National Natural Science Foundation of China (Nos. 22267023).

References

1 a) Champoux J J, *Nucleic Acid Res Mol Biol*, 60 (1998) 111; b) Wang J C, *Nat Rev Mol. Cell Biol*, 3 (2002) 430.

2 a) Thomas C J, Rahier N J & Hecht, S. M, *Bioorg Med Chem,* 12 (2004) 1585; b) Urasaki Y, Laco G, Takebayashi Y, Bailly C, Kohlhagen G & Pommier Y, *Cancer. Res*, 61 (2001) 504; (c) Morrell A, Placzek M, Parmley S, Grella B, Antony S, Pommier S & Cushman M, *J Med Chem*, 50 (2007) 4388; d) Clark R L, Deane F M, Anthony N G, Johnston B F, McCarthy F O & Mackay S P, *Bioorg Med Chem*, 15 (2007) 4741; e) Baldwin E L & Osheroff N, *Curr. Med. Chem*. *Anticancer Agents*. 5 (2005) 363; (f) DeVita V T, Hellman S & Rosenberg S A, *Cancer Principles and Practice of Oncology, 6thed.;* (Lippincott, Williams and Wilkins: Philadelphia, PA) 2001.; g) Minotti G, Menna,P, Salvatorelli E, Cairo G & Gianni L, *Pharmacol Rev*, 56 (2004) 85; h) Goodell J R, Ougolkov A V, Hiasa H, Kaur H, Remmel R, Billadeau D D & Ferguson D M, *J Med Chem,* 51 (2008) 179; i) Fossé P, René B, Charra M, Paoletti C & Saucier J M, *Mol Pharmacol,* 42 (1992) 590.

3 a) Morphy R & Rankovic, Z, *J Med Chem*, 48 (2005) 6523; b) Cavalli A, Bolognesi M L, Minarini A, Rosini M, Tumiatti V, Recanatini M & Melchiorre C, *J Med Chem*, 51 (2008) 347.

4 Corbett K D & Berger J M, *Annu Rev Biophy. Biomol Struct*, 33 (2004) 95.

5 Berger J M, Gambin S J, Harrison S C & Wang J C, *Nature*, 379 (1996) 225.

6 a) Eder J P, Chan V, Wong J, Wong Y, Ara W G, Northey D, Rizvi N &Teicher B A, *Cancer Chemother Pharmacol,* 42 (1998)327; b) Houghton J A, Cheshire P J, Hallman J D II, Lutz L, Luo X, Li Y & Houghton P J, *Clin Cancer Res*, 2 (1996) 107 ; c) Crump M, Lipton J, Hedley D, Sutton D, Shepherd F, Minden M, Stewart K, Beare S & Eisenhauer E, *Leukemia,* 13 (1999) 343; d) Vey N, Kantarjian H, Beran M, O'Brien S, Cortes J, Koller C & Estey E, I*nvest New Drugs*, 17 (1999) 89.

7 a) Simon T, Langler A, Berthold F, Klingebiel T & Hero B T, *J Pediatr Hematol Oncol*, 29 (2007) 101.; b) Choi H J, Cho B C, Shin S J, Cheon S H, Jung J Y, Chang J S, Kim K, Sohn J H & Kim J H, *Can Chem Pharm*, 61 (2008) 309; (c) Saraiya B, Gounder M, Dutta J, Saleem A, Collazo C, Zimmerman L, Nazar A, Gharibo M, Schaar D, Lin Y, Shih W, Aisner J, Strair R K & Rubin E H, 19 (2008) 411.

8 a) Salerno S, Da S, Taliani F, Simorini S F, La Motta C, Fornaciari G & Marini A M, *Curr Med Chem,* 17 (2010) 4270.; b) Utsugi T, Aoyagi K, Asao T, Okazaki S, Aoyagi Y, Sano M, Wierzba K & Yamada Y, *Jpn J Cancer Res*, 88 (1997) 992.; c) Barret J M, Cadou M & Hill B T, *Biochem Pharm*, 63 (2002) 251.; d) Via L D, Magno S M, Gia O, Marini A M, Da Settimo F, Salerno S, La Motta C, Simorini C F, Taliani S, Lavecchia A, Di Giovanni C, Brancato G, Barone V & Novellino E, *J Med Chem*, 52 (2009) 5429.; e) Nabiev I, Chourpa I, Riou J F, Nguyen C H, Lavelle F & Manfait M, *Biochemistry*, 33 (1994) 9013; f) Finlay G J, Riou, J. F & Baguley B C, *Eur J Can*, 32A (1996) 708.; g) Wang B, Perchellet E, Wang Y, Tamura M, Hua D H & Perchellet J P H, *Anti Can Drugs* 14 (2003) 503.

9 a) Du K J, Wang J Q, Kou J F, Li G Y, Wang L L, Chao H & Ji L N*, Eur J Med Chem*, 46 (2011) 1056.; b) Kou J F, Qian C, Wang J Q, Chen X, Wang L L, Chao, H & Ji L N, *J Biol Inorg Chem,* 17 (2012) 81.; c) Zhang P Y, Wang J Q, Huang H Y, Qiao L P, Ji L N & Chao H, *Dalton Trans*, 42 (2013) 8907.; d) Wang Y C, Qian C, Peng Z L, Hou X J, Wang L L, Chao H & Ji L N, *J Inorg Biochem*, 130 (2014) 15 ; e) Xiong K, Qian C, YuanY X, Wei L, Liao X. X, He L T, Rees T W, Chen Y, Wan J, Ji L N & Chao H, *Angew Chem Int Ed*, 59 (2020) 16631 ; f) Du K J, Liang J W, Wang Y, Kou J F, Qian C, Ji L N & Chao H, *Dalton Trans*, 43 (2014) 17303.

10 Cohen G & Eisenberg H, *Biopoly*, 8 (1969) 45.

11 Carter M T,Rodriguez M & Bard A, *J Am Chem Soc,* 111 (1989) 8901.

12 Osheroff N, Shelton E R & Brutlag D L, *J Biol Chem*, 258 (1983) 9536.

13 Fortune J M & Osheroff N, *J Biol Chem*, 273 (1998) 17643.

14 Ginouves M, Carme B, Couppie P & Prevot G, *J. clin. microbiol*, 52 (2014) 2131.

15 Kasibhatla S, Amarante-Mendes G P, Finucane D, Brunner T, Bossy-Wetzel E & Green D R, *Cold. Spring. Harbor. Protocols*, 3(2006) 4493

16 Wang J & Hanan G S, *Syn Lett*, 8(2005) 1251.

17 Collin J P, Guillerez S, Sauvage J P, Barigelletti F, De Cola L, Flamigni L & Balzani V, *Inorg Chem*, 30 (1991) 4230.

18 Ambroise A & Maiya B G, *Inorg Chem*, 39 (2000) 4256.

19 Goulle V, Harriman A & Lehn J M, *J Chem Soc Chem Comm*, (1993) 1034.

20 Satyanarayana S, Dabroniak J C & Chaires J B, *Biochem*, 31 (1992) 9319.

21 Satyanarayana S, Daborusak J C & Chaires J B, *Biochem*, 32 (1993) 2573.

22 Wu J Z, Ye BH, Wang L, Ji L N, Zhou JY, Li R H & Zhou Z Y, *J Chem Soc Dalton. Trans,* (1997) 1395.

23 Gao F, Chao H, Zhou F, Yuan Y X, Peng B & Ji L N, *J Inorg Biochem*, 100 (2006) 1487.

24 Friedman A E, Chambron J C, Sauvage J P, Turro, N J & Barton J K, *J Am Chem Soc*, 112 (1990) 4960.

25 Nair R B,Teng E S, Kirkland S L & Murphy C, *J Inorg Chem*, 37 (1998) 139.

26 LePecq J B & Paoletti C, *J Mol Biol*, 27 (1967) 87.

27 Tselepi-Kalouli E & Katsaros N, *J Inorg Biochem,* 37 (1989) 271.

28 Kumar CV, Asuncion E H , Kumar C V & Asuncion E H, *J Am Chem Soc,* 115 (1993) 8547.
29 Waring M J, *J Mol Biol,* 13 (1965)269.
30 Neyhart G A, Grover N, Smith S R, Kalsbeck W A, Fairley T A, Cory M & Thorp H H, *J Am Chem Soc*, 115 (1993) 4423.
31 Han M J, Duan Z M, Hao Q, Zheng S Z, & Wang K Z, *J Phys Chem C,* 111 (2007) 16577.
32 McGhee J D, *Biopol Orig Res Biomol*, 15 (1976)1345.
33 Chan H L, Liu H Q, Tzeng B C, You Y S, Peng S M, Yang M & Che C M, *Inorg Chem*, 41(2002) 3161.
34 Fortune J M, Velea L, Graves D E, Utsugi T,Yamada Y & Osheroff N, *Biochem,* 38 (1999)15580.
35 Abassi Y A, Xi B, Zhang W, Ye P, Kirstein S L, Gaylord M R & Xu X, *Chem Biol*, 16 (2009)712.
36 Singh N P, McCoy M T, Tice R R & Schneider E L, *Exp Cell Re*s, 175 (1988) 184.
37 Vermes I & Haanen C, *Adv Clin Chem*, 31 (1994) 177.
38 Van Furth R &Van Zwet T L, *J Immunol. Methods*. 108 (1988) 45.
39 Savill J S, Wyllie A H, Henson J E, Walport M J, Henson P M & Haslett C, *J Clin Invest*, 83 (1989) 865 .
40 Thornberry N A & Lazebnik Y, *Science*, 281(1998) 1312
41 Ghobrial I M, Witzig T E & Adjei A A, *Cancer J Clin*, 55 (2005) 178.
42 Vermes I, Haanen C, Steffens-Nakken H & Reutellingsperger C, *J Imm Meth*, 184 (1995) 39.
43 Bhattacharjee R N, Park K S, Kumagai Y, Okada K, Yamamoto M, Uematsu S & Akira S, *J Biol Chem*, 281 (2006) 36897.
44 Suzuki K & Uyeda M, *Biosci Biotech Biochem*, 66 (2002) 1706.
45 Suzuki K, Shono F & Uyeda M, *Biosci Biotech Biochem*, 62 (1998) 2073.
46 Fortune J M, Velea L, Graves D E, Utsugi T, Yamada Y & Osheroff N, Biochemistry. 38 (1999)15580.
47 A) Gao F, Chao H, Wang J Q, Yuan Y X, Sun B, Wei Y F & Ji L N, *J Biol Inorg Chem,* 12 (2007) 1015.; b) Gao F, Chao H, Zhou F, Chen X, Wei Y F & Ji L N, *J Inorg Biochem*, 102 (2008) 1050.